A Joint Design of Platoon Communication and Control Based on LTE-V2V

Chunhua Hong, Hangguan Shan, Meiyan Song, Weihua Zhuang, Zhiyu Xiang, Yingxiao Wu, Xiaoli Yu

***Abstract*—Recently, vehicle platooning has attracted a lot of attention as one of the promising solutions to the explosion of vehicle numbers. By exchanging information among vehicles through communication networks, vehicle platooning can significantly improve traffic safety and efficiency. In this paper, we develop a joint systematic design of platoon communication and control to reduce position errors of consecutive vehicles and to improve platoon safety. Through separate information dissemination of the platoon leader and followers, we improve the success probability of the platoon leader's information dissemination. To extend the communication range of the platoon leader and also the platoon scale, we propose to use relays to forward the platoon leader's messages. Further, an adaptive distributed model predictive control (DMPC) based controller is presented, which can adjust its control parameters according to platoon state and dynamic information sources. Simulation results not only verify the proposed systematic design in terms of position errors, but also show that our scheme performs well in vehicle failure cases where collisions can be avoided and platoon safety improved.**

***Index Terms*—Vehicle platooning, vehicular network, intra-platoon communications, distributed model predictive control.**

I. Introduction

Rapidly-growing vehicular traffic has caused serious problems, such as traffic accidents, congestion, and exhaust emissions. Platooning provides an effective solution, in which autonomous vehicles in the same lane are grouped into platoons. Vehicles in a platoon move at the same speed and maintain a small constant distance gap from preceding vehicles [1]–[3]. To maintain a safe and efficient platoon, vehicles in the platoon have to obtain kinetic status information, such as position and velocity, from other vehicles. In early research, the information is obtained through sensors such as radar [4], [5]. However, such sensors are limited to the range of visibility and are heavily affected by the weather. More recently, vehicular communication is introduced to facilitate information exchange among vehicles, and shows its benefits.

In platooning, an efficient inter-vehicle communication (IVC) protocol is needed to deliver control messages. For IVC protocol design, the dissemination of periodic beacon messages and event-driven safety messages has been extensively studied [6]–[9]. Moreover, some advanced IVC protocols are proposed specifically for vehicle platoon scenarios [10]–[13]. On the other hand, it is necessary to have an advanced platoon control mechanism. In recent years, some advanced platoon control laws have been proposed, including cooperative adaptive cruise control (CACC) [14], sliding-mode control (SMC) [15], [16], H_∞ control [17], [18], and model predictive control (MPC) [19], [20]. Meanwhile, other issues such as the communication network topology, vehicle dynamics, and formation geometry (i.e., the desired inter-vehicle distance) are investigated [21], [22]. However, the aforementioned studies focus only on either platoon communication or platoon control. For platoon communication-related works, the existing IVC protocols aim at improving communication performance, while neglecting the requirements of platoon control. As for platoon control, most existing studies present control strategies under certain communication network topologies without taking account of communication failures caused by the time-varying channel.

There are works on solutions of systematic platoon communication and control design, mostly for a one-hop platoon where the platoon leader is accessible to all vehicles [23]–[25]. When direct communication between the platoon leader and its followers fails, the followers need to estimate the leader's status. Hence, improvement of platoon control performance is severely restricted to the communication environment. Moreover, the platoon scale is limited to the maximal one-hop communication range.

In this paper, we study a joint system of periodic platoon communication and control to reduce position errors and improve platoon safety. Specifically, we propose a communication scheme based on LTE vehicle-to-vehicle (LTE-V2V) communication, which consists of two phases, i.e., the leader's information dissemination (LID) and the followers' information dissemination (FID). We use relays to forward the leader's messages in the LID phase, and adopt frequency reuse (i.e., one sub-channel is allocated to multiple vehicles) to improve spectrum utilization in the FID phase. Further, we extend an adaptive control strategy using a modified distributed model predictive control (DMPC) method, where the control parameters are adjusted according to platoon state (i.e., whether any vehicle in the platoon is in an abnormal state) and dynamic information sources (i.e., the set of vehicles whose messages are successfully received) dependent on the time-varying wireless channel. To further improve the platoon safety, auxiliary methods of communication are employed.

C. Hong, H. Shan, M. Song, and Z. Xiang are with the College of Information Science and Electronic Engineering and with Zhejiang Provincial Key Laboratory of Information Processing and Communication Networks, Zhejiang University, Hangzhou, 310027 China (e-mail: {hshan, hongch, songmy, xiangzy}@zju.edu.cn).

W. Zhuang is with the Department of Electrical and Computer Engineering, University of Waterloo, Waterloo, N2L 3G1 Canada (e-mail: wzhuang@uwaterloo.ca).

Y. Wu is with Zhejiang Laboratory, Hangzhou, 310000 China (e-mail: wuyx@zhejianglab.com).

X. Yu is with the College of Energy Engineering, Zhejiang University, Hangzhou, 310027 China (e-mail: yuxl@zju.edu.cn).

Finally, we conduct simulations to analyze the effects of communication on platoon control from several aspects and to validate the platoon safety in both vehicle normal and failure cases. The contributions of this paper are summarized as follows:

- Through the proposed periodic communication and control, the influence of communication delay can be alleviated. The reliability of LID is improved and platoon scale is extended by appropriately selecting relays, and the duration of FID can be shortened with frequency reuse. Thus, the reaction time of vehicles to collect information and adjust their driving status is reduced;
- The adaptive DMPC-based control strategy enables vehicles to fully use the information received from other members to better follow the platoon leader and cope with an emergent case due to vehicle failures. In addition, to improve platoon safety, we design the control strategy by integrating a constraint to maintain a safe distance gap with the closest vehicles. Additionally, the proposed auxiliary methods enhance the ability of resisting communication failures;
- Simulation results show the effectiveness of our proposed joint design in guaranteeing platoon safety in both vehicle normal and failure cases where position errors are well controlled and vehicle collisions can be avoided successfully. Furthermore, comparison with C-V2X Mode 4 shows the benefit of the proposed relay-based communication scheme in terms of keeping a more reliable connection to the platoon leader for platoon members, thus improving the platoon control performance.

The remainder of this paper is organized as follows. In Section II, we discuss related works on platoon communication and control. In Section III, we describe the system model. In Section IV, the relay selection problem is studied. Our adaptive control strategy is presented in Section V. Finally, we validate our proposed solutions through extensive simulations in Section VI, followed by concluding remarks in Section VII.

II. Related Work

In the past decades, there are many research works on platoon communication. In [15], Fernandes and Nunes propose intra-platoon information management strategies for dealing with safe and stable operation, arguing that using anticipatory information from both the platoon leader and the followers significantly improves platoon string stability. Peng *et al*. [26] jointly consider the evolved multimedia broadcast multicast services (MBMS) and device-to-device (D2D) multicast communications to enable intra-platoon communications, where a sub-channel allocation scheme and a power control mechanism are proposed. In [27], an IEEE 802.11p-based communication model is introduced for multiplatoon scenarios, with a probabilistic performance analysis of distributed-coordination-function-based intra- and inter-platoon communications.

In addition, platoon control mechanisms have been extensively studied. Oncu *et al*. [14] propose a CACC system to improve traffic flow stability and throughput using a constant-time headway spacing policy. In [17], a multiobjective H_∞ control formulation is investigated for adaptive cruise control (ACC) and CACC structures to guarantee the stability of a vehicle platoon. The proposed control strategy is to provide not only the system stability, but also the string stability as distinct from the traditional H_∞ control. In [28], a sliding-mode based control law is studied to guarantee both homogeneous and heterogeneous string stability, in which a constant-time headway spacing policy is applied and the parasitic time delays and lags of the actuators and sensors are considered. Furthermore, considering fixed yet unidirectional communication network topologies, Zheng *et al*. [29] present a DMPC method that does not need all followers to maintain connections with the platoon leader. However, the impact of packet drops due to the time-varying wireless channel and potential interference is not explored.

More recently, research efforts are extended to jointly deal with both communication and control of a vehicle platoon [23]–[25]. In [23], a joint control-communication scheme is developed for a practical traffic scenario based on IEEE 802.11p. The contention-based communication scheme results in communication congestion and performance degradation, especially for a crowded scenario with a large and uncertain communication delay. Zhang *et al*. [24] propose an LTE-V2V assisted platooning system, where a prediction-based control scheme is used to reduce the required intra-platoon gap. In [25], the control parameter setting of vehicles and radio resource allocation in an LTE-V2V network for cooperative awareness message (CAM) transmission are jointly considered to minimize position tracking error, while guaranteeing the reliability requirements of V2V communication and string stability of the platoon with a preceding-leader-following topology. Different from most of the existing studies focusing on one-hop communication range and fixed communication network topologies in a normal platoon state, in this paper, we use relays to extend communication range and design an adaptive control strategy that can resist channel impairment (thus fitting time-varying communication network topologies) and deal with an abnormal platoon state due to vehicle failures as well.

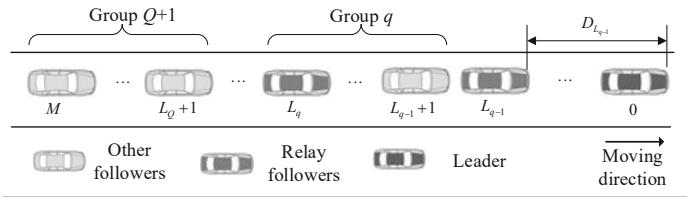

Figure 1. Platoon scenario and vehicle grouping.

III. System Model

In this section, we introduce the vehicle platoon scenario as well as communication and control models. Consider a platoon of $M+1$ vehicles driving in the same lane, as illustrated in Fig. 1. Label the vehicles as $0, 1, ..., M$, where Vehicle 0 is the leader of the platoon and the others are followers. Each vehicle is equipped with an embedded global positioning

Table I
SUMMARY OF IMPORTANT SYMBOLS

Symbol	Definition
α	Path loss exponent
B	Number of sub-channels in FID
$c_{m,\mathrm{a}}$	Comfort coefficient of Vehicle m
$c_{m,j}$	Importance coefficient of Vehicle j for Vehicle m
$c_{m,\mathrm{u}}$	Convincing coefficient of Vehicle m
D_{c}	Constant gap of adjacent vehicles
M	Number of following vehicles
N	Length of a prediction window
N_{LID}	Number of slots reserved for LID
N_{FID}	Number of slots reserved for FID
N_q	Number of slots reserved for Relay q
P_{t}	Transmit power
$\mathcal{S}_m(t)$	Set of vehicles from which Vehicle m receives control messages in $[t, t+T]$
T	Frame duration
T_{s}	Slot duration
$u_m^{\mathrm{a}}(k\|t)$	kth assumed control input of Vehicle m at time t
$u_m^{\mathrm{p}}(k\|t)$	kth predicted control input of Vehicle m at time t
$u_{m,\max}(t)$	Maximum acceleration of Vehicle m at time t
$u_{\min}$	Maximum negative breaking acceleration
u_0	Maximum acceleration when vehicle velocity is 0
u_{th}	Maximum acceleration when vehicle velocity is v_{th}
v_{th}	Maximum velocity of vehicles
W	Bandwidth of intra-platoon communication
$\mathbf{y}_m(t)$	Kinetic status of Vehicle m at time t
$\mathbf{y}_m^{\mathrm{a}}(k\|t)$	kth assumed kinetic status of Vehicle m at time t
$\mathbf{y}_m^{\mathrm{p}}(k\|t)$	kth predicted kinetic status of Vehicle m at time t
$\bar{\mathbf{y}}_{m,j}(k\|t)$	kth ideal kinetic gap between Vehicles m and j at time t

system (GPS) device and other sensors to acquire its own driving status (e.g., position, velocity, acceleration, and failure indication). To extend the communication range of the platoon leader, there are Q relays to forward the leader's information, labeled as $L_1, L_2, ..., L_Q$, whose distances from the leader are denoted as $D_{L_1}, D_{L_2}, ..., D_{L_Q}$, respectively. The whole platoon is thus divided into $Q+1$ groups, with Group q consisting of Vehicles $\{L_{q-1}+1, L_{q-1}+2, ..., L_q\}$, where $q \in \{1, 2, ..., Q+1\}$. Specifically, we let Vehicle L_0 and Vehicle L_{Q+1} represent Vehicle 0 and Vehicle M, respectively. In this work, we consider only longitudinal control. A summary of important symbols is given in Table I for easy reference.

The platoon system operates under periodic control, in which time is partitioned into frames of constant duration T, as shown in Fig. 2. Each frame consists of multiple slots, each of duration T_{s}. Let the total radio spectrum bandwidth allocated to the platoon be W, and the transmit power of all vehicles be P_{t}. At the beginning of each frame, vehicles sample their driving status, which will be transmitted in the current frame to other vehicles for calculating their control inputs. Each frame is divided into two phases. In the first phase, vehicles within the same platoon exchange information with each other (named intra-platoon communication). The exchanged information and bandwidth or sub-channel allocation to facilitate intra-platoon communication are specified later in Subsection III-C. In the second phase, computation (i.e., vehicles calculating the control inputs for the next multiple frames based on the received information) and inter-platoon communication (e.g., for management between platoons) take place simultaneously. Though inter-platoon communication is beyond the scope of this paper, for extension convenience, it is included in the communication module. It is noteworthy that the division of time resource between intra-platoon communication and inter-platoon communication should depend on the size of messages transmitted in both phases, bandwidth allocation for a platoon, and spectrum efficiency supported by the physical layer. In this work, to study the effect of the proposed joint design of platoon communication and control, we will consider in Section VI a frame of long enough duration to accommodate the potential size of messages in both phases. However, the detailed message and control design for inter-platoon management is considered as future work.

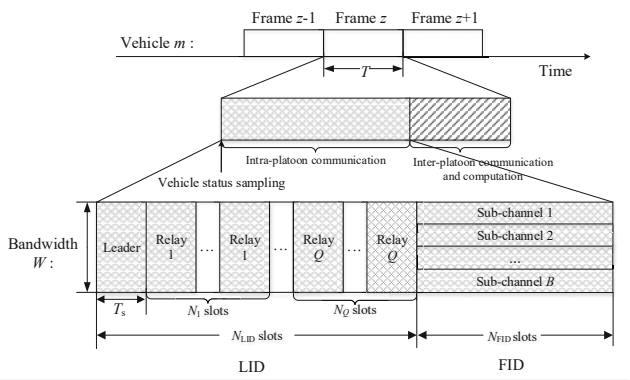

Figure 2. Communication frame structure and functionality.

A. Vehicle Dynamics

The model of vehicle dynamics captures the relationship between vehicle kinetic status and control variables. The control variable is specified as acceleration, and the kinetic status consists of vehicle position and velocity. The discrete-time dynamics model for Vehicle m is

$$x_m(t+1) = x_m(t) + v_m(t)T + 0.5u_m(t)T^2 \tag{1a}$$

$$v_m(t+1) = v_m(t) + u_m(t)T \tag{1b}$$

where $x_m(t)$ and $v_m(t)$ denote the position and velocity of Vehicle m at time t, respectively, T is the frame duration, and $u_m(t)$ is Vehicle m's control input, i.e., its desired acceleration. The control input is subject to a box constraint

$$u_{\min} \le u_m(t) \le u_{m,\max}(t) \tag{2}$$

where $u_{\min}$ is the minimal acceleration (i.e., the maximal negative braking acceleration) and is a constant, and $u_{m,\max}(t)$ is the maximal acceleration of Vehicle m at time t satisfying

$$u_{m,\max}(t) = \frac{F_{\max} - f_{\mathrm{e}} m_{\mathrm{v}} g - f_{\mathrm{a}} v_m^2(t)}{m_{\mathrm{v}}} \tag{3}$$

with g, $F_{\max}$, m_{v}, f_{a}, and f_{e} denoting the acceleration of gravity, maximal vehicle traction, vehicle mass, air resistance coefficient, and friction resistance coefficient, respectively. We assume that vehicles in the platoon are isomorphic, i.e., all the vehicles have the same dynamic parameters.

Further, let vector $\mathbf{y}_m(t) = [x_m(t), v_m(t)]^{\mathrm{T}}$ denote the kinetic status of Vehicle m at time t, so that (1) can be rewritten as:

$$\mathbf{y}_m(t+1) = \mathbf{F}_{\mathrm{d}}[\mathbf{y}_m(t), u_m(t)] = \begin{bmatrix} 1 & T \\ 0 & 1 \end{bmatrix} \begin{bmatrix} x_m(t) \\ v_m(t) \end{bmatrix} + \begin{bmatrix} \frac{T^2}{2} \\ T \end{bmatrix} u_m(t) \quad (4)$$

where matrix $\mathbf{F}_{\mathrm{d}}[\cdot,\cdot]$ denotes the vehicle dynamics function.

B. Objective of Platoon Control

The objective of platoon control is to let the followers track the leader's speed, while maintaining a desired constant distance gap D_{c} between adjacent vehicles. The constant spacing condition is satisfied as

$$\lim_{t\to\infty} |v_m(t) - v_0(t)| = 0 \quad (5a)$$

$$\lim_{t\to\infty} |x_0(t) - x_m(t) - mD_{\mathrm{c}}| = 0. \quad (5b)$$

In the case of communication failures with the leader, the followers' information can be used because they follow the control objective as well. However, the followers' information is less valuable than the leader's because of communication delay, reaction delay, and influence of neighboring vehicles.

C. Intra-platoon Communication

To improve platoon control performance, an effective intra-platoon communication protocol is needed. Considering the limited radio spectrum resources, we focus on transmitting information that improves the platoon control performance rather than delivering each vehicle's information fairly. Fig. 2 illustrates our intra-platoon communication scheme, consisting of the LID and the FID. Based on LTE-V2V, the communication resources allocated to both the LID and FID are divided into slots and sub-channels, and each vehicle uses pre-allocated resource elements for information exchange.

Since the platoon leader is responsible for platoon management and its driving status is the control reference of the followers, we separate the LID from the FID to eliminate interference and to improve the probability of successfully receiving the leader's messages. As shown in Fig. 2, there are N_{LID} slots in total allocated for the LID, in which the platoon leader uses the first slot to broadcast its information, including its position, velocity, acceleration, and fault indication of any vehicle in the platoon that is in an abnormal state. We consider that if any vehicle in the platoon is in an abnormal state, it will broadcast its state information (i.e., abnormal acceleration or deceleration). Other vehicles overhearing this information will re-broadcast it to notify other members in the platoon. In order to extend the platoon leader's communication range, we use relays to forward the leader's information, using the remaining $(N_{\mathrm{LID}} - 1)$ slots. We consider that, to maximize the benefit of utilizing relays, not only each relay L_q but also the number of slots allocated to a relay N_q should be appropriately decided (see Fig. 2). The relay selection problem will be studied later in Section IV. The platoon leader can be in charge of calculating and disseminating the relay configuration in its platoon leader's information. If a follower vehicle is configured as a relay, it will keep forwarding the platoon leader's information at allocated slots until the relay configuration changes. It is also noteworthy that in the LID phase each vehicle transmits over the whole bandwidth W due to no other simultaneously-transmitting platoon members.

The leader can be out of connection for some followers, e.g., due to severe channel impairments. As a result, as shown in Fig. 2 the FID is to exchange information among neighboring vehicles using N_{FID} slots. In the FID phase, the allocated bandwidth W is divided into B sub-channels, numbered $1, 2, ..., B$. Vehicle m chooses the sub-channel with index equal to the remainder of m divided by B for transmission. When the number of sub-channels B is less than the number of following vehicles M, the frequency reuse within the platoon increases spectrum utilization and improves the information exchange rate. The closer two vehicles are, the higher the probability of successfully exchanging information. The probability also depends on the value of B/M. As B/M increases, the interference within the platoon decreases. Thus, the probability of successful communication with neighboring vehicles increases, leading to better communication performance. However, given W, a larger B value means smaller sub-channel bandwidth, which increases the transmission time. It is also noteworthy that, in the proposed intra-platoon communication scheme, to make each platoon member transmit in the allocated slot(s), all vehicles in a platoon need to keep synchronized, thereby increasing the overhead.

IV. Relay Selection

In the LID phase, we use relays to forward the leader's information. In this section, we propose an approach to select relays and determine their resource allocation, aiming at maximizing the minimal average signal-to-noise ratio (SNR) among the vehicles in the platoon.

In the LID procedure, each vehicle receives messages from the leader and relays in front within the platoon. With the vehicle grouping as depicted in Fig. 1, vehicles in the same group receive the leader's information from the same transmitter(s). Considering a distance-dependent large-scale attenuation channel model, the average SNR decreases as the distance between the transmitter and receiver increases. Consequently, in Group q, Vehicle L_q has the minimal average SNR since it has the largest distance from the transmitters in front. In the whole platoon, the vehicle having the minimal average SNR is among Vehicles $\{L_1, L_2, ..., L_Q, M\}$. To simplify the analysis, we assume the platoon is under an ideal condition, where all consecutive vehicles have the desired distance gap D_{c}, so the distance between Vehicle L_q and the platoon leader satisfies $D_{L_q} = L_q D_{\mathrm{c}}$. Using the maximal-rate-combining (MRC) method and provided that the selected relay Vehicle L_q retransmits for N_q times (see Fig. 2), the average SNR of relays and Vehicle M are given by

$$\bar{\gamma}(L_q) = \sum_{q'=1}^{q-1} \frac{N_{q'} P_{\mathrm{t}} [(L_q - L_{q'}) D_{\mathrm{c}}]^{-\alpha}}{N_0} + \frac{P_{\mathrm{t}} (L_q D_{\mathrm{c}})^{-\alpha}}{N_0} \quad (6a)$$

$$\bar{\gamma}(M) = \sum_{q'=1}^{Q} \frac{N_{q'} P_{\mathrm{t}} [(M - L_{q'}) D_{\mathrm{c}}]^{-\alpha}}{N_0} + \frac{P_{\mathrm{t}} (M D_{\mathrm{c}})^{-\alpha}}{N_0} \quad (6b)$$

where $q \in \{1, 2, ..., Q\}$ is the relay index, α denotes the path-loss exponent, and N_0 represents the received background noise power.

The relay selection is formulated as an integer programming problem:

$$\max_{Q,\{L_q\}_{q=1}^{Q},\{N_q\}_{q=1}^{Q}} \quad \min\{\bar{\gamma}(L_1), \bar{\gamma}(L_2), ..., \bar{\gamma}(L_Q), \bar{\gamma}(M)\} \tag{7a}$$

$$\text{s.t.} \quad 0 < L_1 < L_2 < ... < L_Q < M \tag{7b}$$

$$\sum_{q=1}^{Q} N_q = N_{\mathrm{LID}} - 1 \tag{7c}$$

$$Q \leq \min\{M-1, N_{\mathrm{LID}} - 1\} \tag{7d}$$

$$\bar{\gamma}(L_q) \geq \gamma_{\mathrm{th}}, \forall q \in \{1, 2, ..., Q\} \tag{7e}$$

$$Q, L_q, N_q \in \mathbb{Z}^+, \forall q \in \{1, 2, ..., Q\} \tag{7f}$$

where γ_{th} denotes the SNR threshold to successfully decode the leader's message. The objective function given in (7a) is to maximize the minimal average SNR among all relays and Vehicle M. Constraint (7b) describes the relay order in the platoon. Constraint (7c) means that the total number of slots reserved for the Q selected relays is $N_{\mathrm{LID}} - 1$. Inequality (7d) ensures that the number of selected relays should be no more than the minimum between the number of vehicles in the platoon excluding Vehicle M and the total number of slots reserved for relaying. Constraint (7e) ensures that a vehicle can be a relay only if on average it has high enough SNR to successfully decode the platoon leader's message. Constraints (7f) imply that the optimization problem needs a positive integer solution.

Since the platoon scale cannot be too large, we use a dynamic programming method [30] to solve this problem, as described in Algorithm 1 and Algorithm 2. Algorithm 1 is to find the best relay selection result from all feasible relay selection results in $\mathscr{X}$ produced by Algorithm 2. Algorithm 2 is designed in a recursive manner to search all relay selection results satisfying constraints in (7b)-(7f).

Algorithm 1 RelaySelection

Input: $M, N_{\mathrm{LID}}, P_{\mathrm{t}}, \gamma_{\mathrm{th}}, D_{\mathrm{c}}, N_0, \alpha$

Output: The best relay selection result $Q^*, \{L_q^*\}_{q=1}^{Q^*}, \{N_q^*\}_{q=1}^{Q^*}$

$\mathbf{x} \leftarrow$ zeros(1, M);
$\mathscr{X} \leftarrow$ RelaySearching($\mathbf{x}$, 1, $M-1$, N_{LID}, γ_{th});
$\gamma_{\max} \leftarrow 0$;
for each $\mathbf{x}$ in $\mathscr{X}$ **do**
  $q \leftarrow 1$;
  for each $i = 1 : M-1$ **do**
    if $\mathbf{x}[i] > 0$ **then**
      $N_q \leftarrow \mathbf{x}[i]$;
      $L_q \leftarrow i$;
      $q \leftarrow q + 1$;
    end if
  end for
  $Q \leftarrow q$;
  Calculate $\bar{\gamma}(L_1), \bar{\gamma}(L_2), ..., \bar{\gamma}(L_Q), \bar{\gamma}(M)$ according to the relay selection result $Q, \{L_q\}_{q=1}^{Q}, \{N_q\}_{q=1}^{Q}$;
  $\gamma_{\min} \leftarrow \min\{\bar{\gamma}(L_1), \bar{\gamma}(L_2), ..., \bar{\gamma}(L_Q), \bar{\gamma}(M)\}$;
  if $\gamma_{\min} \geq \gamma_{\max}$ **then**
    $\gamma_{\max} \leftarrow \gamma_{\min}$;
    $(Q^*, \{L_q^*\}_{q=1}^{Q^*}, \{N_q^*\}_{q=1}^{Q^*}) \leftarrow (Q, \{L_q\}_{q=1}^{Q}, \{N_q\}_{q=1}^{Q})$;
  end if
end for

Algorithm 2 RelaySearching

Input: $\mathbf{x}, s_{\mathrm{v}}, e_{\mathrm{v}}, N_{\mathrm{LID}}, \gamma_{\mathrm{th}}$

Output: The set of all feasible relay selection results $\mathscr{X}$

$\mathscr{X} \leftarrow \{\}$;
if $N_{\mathrm{LID}} - 1 < 0$ or $s_{\mathrm{v}} > e_{\mathrm{v}}$ **then**
  return;
end if
if $N_{\mathrm{LID}} - 1 = 0$ **then**
  $\mathscr{X} \leftarrow \{\mathbf{x}\}$;
  return;
end if
Calculate the average SNR $\gamma_{s_{\mathrm{v}}}$ of Vehicle s_{v} according to the relay selection result in $\mathbf{x}$;
if $\gamma_{s_{\mathrm{v}}} \geq \gamma_{\mathrm{th}}$ **then**
  for each $i = 0 : N_{\mathrm{LID}} - 1$ **do**
    $\mathbf{x}' \leftarrow \mathbf{x}$;
    $\mathbf{x}'[s_{\mathrm{v}}] \leftarrow i$;
    $\mathscr{X}' \leftarrow$ RelaySearching($\mathbf{x}', s_{\mathrm{v}}+1, e_{\mathrm{v}}, N_{\mathrm{LID}}-i, \gamma_{\mathrm{th}}$);
    $\mathscr{X} \leftarrow \mathscr{X} \cup \mathscr{X}'$;
  end for
else
  return;
end if

V. DMPC-Based Platoon Control Strategy

A platoon control strategy determines how to calculate the vehicles' control inputs in future frames. In this section, we present a platoon control strategy using a modified DMPC model. This control scheme is distributed, being carried out independently by each vehicle. Different from the traditional DMPC method [29], here the control parameters of a vehicle in the platoon are designed to be adaptive according to platoon state (i.e., whether any vehicle in the platoon is in an abnormal state) and dynamic information sources (i.e., the set of vehicles whose messages are successfully received). Furthermore, we take vehicle acceleration as the control input, and add safe distance constraints to cope with occasional vehicle failures. We also adopt auxiliary methods to improve platoon safety in case of failed communications. In the following, we take Vehicle m as an example to present the control strategy.

As shown in Fig. 3, Vehicle m predicts the control inputs in the N frames following the current frame. These N frames are called the prediction window. Focusing on time t, we define two types of Vehicle m's kinetic status consisting of its position and velocity over the prediction horizon $[t+T, t+(N+1)T]$: $\mathrm{y}_m^{\mathrm{p}}(k|t)$, the predicted kinetic status of Vehicle m at time $t+kT$ estimated in the frame starting at time t according to the vehicle dynamics function (4), which depends on the actual status, i.e., $\mathrm{y}_m(t)$ and $u_m(t)$, and the predicted control inputs to be calculated, i.e., $u_m^{\mathrm{p}}(k|t), k = 1, 2, ..., N$; $\mathrm{y}_m^{\mathrm{a}}(k|t)$,

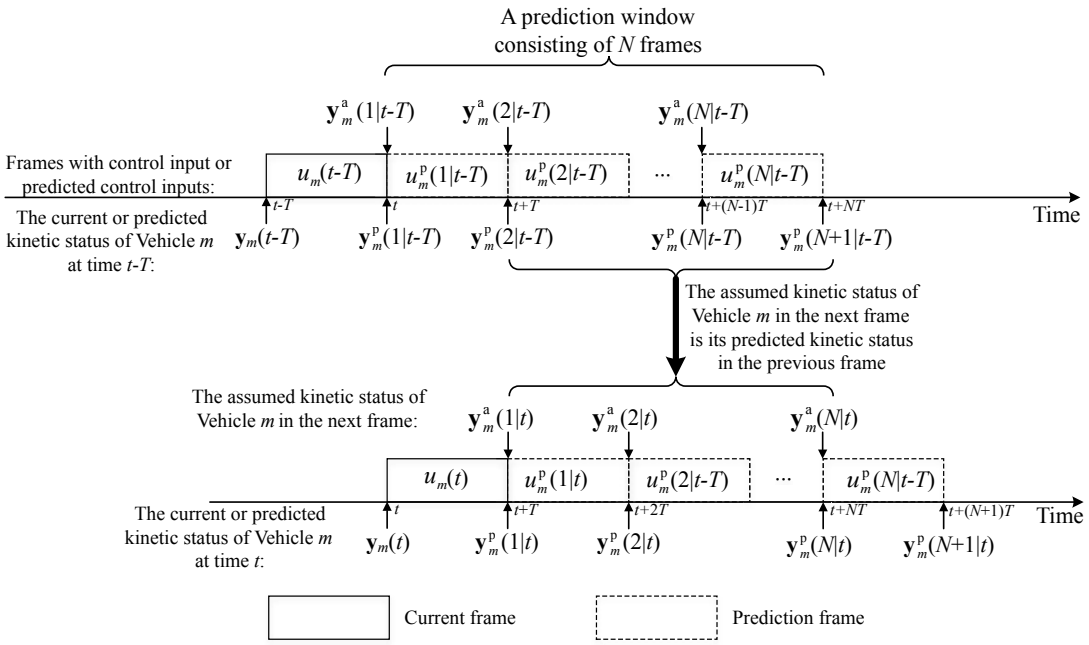

Figure 3. DMPC controller.

the assumed kinetic status of Vehicle m at time $t+kT$, which is a shifted version of the predicted kinetic status calculated in the frame starting at time $t-T$. Specifically, the first and following predicted kinetic status at time $t-T$ are the actual and the assumed kinetic status at time t, respectively, i.e.,

$$\mathbf{y}_m(t) = \mathbf{y}_m^{\mathrm{p}}(1|t-T) \tag{8a}$$

$$\mathbf{y}_m^{\mathrm{a}}(k|t) = \mathbf{y}_m^{\mathrm{p}}(k+1|t-T),\ k \in \{1,2,...,N\}. \tag{8b}$$

The assumed kinetic status $\mathbf{y}_m^{\mathrm{a}}(k|t)$ is transmitted to other vehicles for control. Similarly, Vehicle m receives other vehicles' assumed kinetic status $\mathbf{y}_{j\in\mathcal{S}_m(t)}^{\mathrm{a}}(k|t)$, where $\mathcal{S}_m(t)$ represents the set of vehicles from which Vehicle m successfully receives messages in frame $[t, t+T]$. According to the platoon control objective, each vehicle tracks the speed of the leader and maintains a desired distance gap with the preceding vehicle. Due to possible communication failures with the leader and platoon safety requirements, neighboring vehicles' kinetic status should also be taken into consideration. We assign adaptive weighting factors to different vehicles in order to adjust their effectiveness. In this model, the platoon control objective function is applied to the entire prediction window. Then, the control strategy can be formulated as an optimization problem to keep a desired status (i.e., the same speed and desired distance gap) with other vehicles. In the following subsections, we introduce the objective function and constraints of the optimization problem, respectively.

A. Objective Function

Considering the uncertainty of obtaining the leader's information, we take the other vehicles' kinetic status into account. Actually, the received messages from all member vehicles are used, which is our proposed "ALL" topology. Define $\bar{\mathbf{y}}_{m,j}(t) = [(m-j)D_{\mathrm{c}}, 0]^{\mathrm{T}}$ as the desired kinetic status gap between Vehicles m and j. Since each vehicle's information has a different influence on the platoon control, we assign coefficients to distinguish the importance degree. Thus, the objective function of the kinetic trajectory is expressed as

$$\min_{u_m^{\mathrm{p}}(1|t),\ldots,u_m^{\mathrm{p}}(N|t)} f_1 = \sum_{k=1}^{N}\left[\sum_{j\in\mathcal{S}_m(t)} c_{m,j}||\mathbf{y}_m^{\mathrm{p}}(k|t) - \mathbf{y}_j^{\mathrm{a}}(k|t) - \bar{\mathbf{y}}_{m,j}(k|t)||_2\right] \tag{9}$$

where $c_{m,j}$ is the weighting factor of Vehicle j for Vehicle m.

To ensure driving comfort, the acceleration of vehicles should be close to zero, i.e.,

$$\min_{u_m^{\mathrm{p}}(1|t),\ldots,u_m^{\mathrm{p}}(N|t)} f_2 = \sum_{k=1}^{N}\left[c_{m,\mathrm{a}}|u_m^{\mathrm{p}}(k|t)|\ \right] \tag{10}$$

where $c_{m,\mathrm{a}}$ is the comfort coefficient of Vehicle m.

Further, the predicted kinetic status should be close to the assumed kinetic status since that is used by other vehicles for control. So the following function should also be included in the objective function

$$\min_{u_m^{\mathrm{p}}(1|t),\ldots,u_m^{\mathrm{p}}(N|t)} f_3 = \sum_{k=1}^{N}\left[c_{m,\mathrm{u}}||\mathbf{y}_m^{\mathrm{p}}(k|t) - \mathbf{y}_m^{\mathrm{a}}(k|t)||_2\ \right] \tag{11}$$

where $c_{m,\mathrm{u}}$ denotes the confidence coefficient of Vehicle m.

B. Constraints

1) Velocity Constraint: On real roads, vehicle speeds are restricted. Let v_{th} denote the restricted maximal speed threshold. Then the kth predictive velocity of Vehicle m at time t is constrained as

$$0 \le v_m^{\mathrm{p}}(k|t) \le v_{\mathrm{th}}. \tag{12}$$

To ensure platoon stability and safety, the velocities of adjacent vehicles are under box constraints

$$\begin{aligned} v_{m-1}^{\mathrm{a}}(k|t)-\epsilon \le v_m^{\mathrm{p}}(k|t) \le v_{m-1}^{\mathrm{a}}(k|t)+\epsilon \\ v_{m+1}^{\mathrm{a}}(k|t)-\epsilon \le v_m^{\mathrm{p}}(k|t) \le v_{m+1}^{\mathrm{a}}(k|t)+\epsilon \end{aligned} \tag{13}$$

where $\epsilon \ge 0$ is the allowed velocity difference boundary with adjacent vehicles.

2) Acceleration Constraint: According to Subsection III-A, the kth predictive acceleration constraint of Vehicle m at time t is given by

$$u_{\min} \le u_m^{\mathrm{p}}(k|t) \le u_{m,\max}(k|t) = \frac{F_{\max} - f_{\mathrm{e}} m_{\mathrm{v}} g - f_{\mathrm{a}}[v_m^{\mathrm{p}}(k|t)]^2}{m_{\mathrm{v}}}. \tag{14}$$

3) Safe Distance Constraint: In the platoon control, safety has the highest priority. Safety is guaranteed by keeping a distance gap large enough for reaction (i.e., decelerate or accelerate). Define $d_{m,\mathrm{f}}$ ($d_{m,\mathrm{b}}$) as the forward (backward) safe distance representing the minimal distance that Vehicle m can react to by decelerating (accelerating) to avoid collision with the preceding (following) vehicle when it suddenly brakes (accelerates). The safe distance constraint is applied throughout the prediction window, given by

$$\begin{aligned} & x_{m-1}^{\mathrm{a}}(k|t) - x_m^{\mathrm{p}}(k|t) \ge d_{m,\mathrm{f}} \\ =& 2T v_m^{\mathrm{p}}(k|t) + \frac{[v_{m-1}^{\mathrm{a}}(k|t)]^2 - [v_m^{\mathrm{p}}(k|t)]^2}{2u_{\min}} \end{aligned} \tag{15a}$$

$$\begin{aligned} & x_m^{\mathrm{p}}(k|t) - x_{m+1}^{\mathrm{a}}(k|t) \ge d_{m,\mathrm{b}} \\ =& 2T[v_{\mathrm{th}} - v_m^{\mathrm{p}}(k|t)] \\ & + F_{\mathrm{a},x}[v_{m+1}^{\mathrm{a}}(k|t), v_{\mathrm{th}}] - F_{\mathrm{a},x}[v_m^{\mathrm{p}}(k|t), v_{\mathrm{th}}] \\ & + \{F_{\mathrm{a},t}[v_m^{\mathrm{p}}(k|t), v_{\mathrm{th}}] - F_{\mathrm{a},t}[v_{m+1}^{\mathrm{a}}(k|t), v_{\mathrm{th}}]\} v_{\mathrm{th}} \end{aligned} \tag{15b}$$

where $F_{\mathrm{a},x}[v_{\mathrm{s}}, v_{\mathrm{e}}]$ represents the vehicles' accelerating distance from start velocity v_{s} to end velocity v_{e} with maximal acceleration, and $F_{\mathrm{a},t}[v_{\mathrm{s}}, v_{\mathrm{e}}]$ represents the associated accelerating time in the process. A detailed derivation is given in Appendix A.

4) Convergence Constraint: To make the control process convergent, similar to [29], the following equality constraint is considered:

$$\mathbf{y}_m^{\mathrm{p}}(N+1|t) = \frac{\sum_{j\in\mathcal{S}_m(t)} c_{m,j}\left[\mathbf{y}_j^{\mathrm{a}}(N+1|t) - \bar{\mathbf{y}}_{m,j}(N+1|t)\right]}{\sum_{j\in\mathcal{S}_m(t)} c_{m,j}}. \tag{16}$$

This means that Vehicle m has the same output kinetic status as the weighted average of the assumed kinetic outputs of vehicles in $\mathcal{S}_m(t)$.

C. Controller Design

Finally, the control strategy of each vehicle is specified as

$$\min_{u_m^{\mathrm{p}}(1|t),\ldots,u_m^{\mathrm{p}}(N|t)} f_1 + f_2 + f_3 \tag{17a}$$

$$\text{s.t.} \quad \mathbf{y}_m^{\mathrm{p}}(k|t) = [x_m^{\mathrm{p}}(k|t), v_m^{\mathrm{p}}(k|t)]^{\mathrm{T}} \tag{17b}$$

$$\mathbf{y}_m^{\mathrm{p}}(k+1|t) = \mathbf{F}_{\mathrm{d}}[\mathbf{y}_m^{\mathrm{p}}(k|t), u_m^{\mathrm{p}}(k|t)] \tag{17c}$$

and (12)-(16) hold.

In the optimization problem, constraints (14) and (15) are not convex. To address the optimization problem efficiently, we reformulate it to a convex problem as follows.

For the acceleration constraint (14), $u_{m,\max}(k|t)$ is a convex function of $v_m^{\mathrm{p}}(k|t)$. Due to the property of a convex function and the velocity constraint, we have

$$u_{m,\max}(k|t) \ge \frac{u_{\mathrm{th}} - u_0}{v_{\mathrm{th}}} v_m^{\mathrm{p}}(k|t) + u_0, \quad v_m^{\mathrm{p}}(k|t) \in [0, v_{\mathrm{th}}] \tag{18}$$

where $u_0 = \frac{F_{\max} - f_{\mathrm{e}} m_{\mathrm{v}} g}{m_{\mathrm{v}}}$ and $u_{\mathrm{th}} = \frac{F_{\max} - f_{\mathrm{e}} m_{\mathrm{v}} g - f_{\mathrm{a}} v_{\mathrm{th}}^2}{m_{\mathrm{v}}}$ denote the maximal acceleration when velocity $v_m^{\mathrm{p}}(k|t)$ is 0 and v_{th}, respectively. According to (18), we use the following necessary condition to replace (14):

$$u_{\min} \le u_m^{\mathrm{p}}(k|t) \le \frac{u_{\mathrm{th}} - u_0}{v_{\mathrm{th}}} v_m^{\mathrm{p}}(k|t) + u_0. \tag{19}$$

As for the safe distance constraints in (15), we reformulate them by using the linear yet strict inequalities derived in Appendix B as follows

$$\begin{aligned} x_{m-1}^{\mathrm{a}}(k|t) - x_m^{\mathrm{p}}(k|t) \ge & 2T v_m^{\mathrm{p}}(k|t) - \frac{2v_{m-1}^{\mathrm{a}}(k|t)\epsilon + \epsilon^2}{2u_{\min}} \\ x_m^{\mathrm{p}}(k|t) - x_{m+1}^{\mathrm{a}}(k|t) \ge & 2T[v_{\mathrm{th}} - v_m^{\mathrm{p}}(k|t)] \\ & + \frac{1}{A}[v_m^{\mathrm{p}}(k|t) - v_{m+1}^{\mathrm{a}}(k|t)] \\ & - \frac{u_{\mathrm{th}}}{A^2}\left(\ln\left\{\frac{A}{u_0}[v_{m+1}^{\mathrm{a}}(k|t) - \epsilon] + 1\right\}\right. \\ & \left. - \ln[\frac{A}{u_0} v_{m+1}^{\mathrm{a}}(k|t) + 1]\right) \end{aligned} \tag{20}$$

where $A = \frac{u_{\mathrm{th}} - u_0}{v_{\mathrm{th}}}$. As a result, the optimization problem is transformed to a convex optimization problem. It is noteworthy that, although the transformation is not equivalent, the feasible region of the transformed problem is within that of the original problem and the new problem can be solved efficiently with many existing algorithms such as gradient descent [31].

D. Auxiliary Methods of Communication

Severe communication conditions can cause communication failures even between consecutive vehicles. To acquire reliable status information of neighboring vehicles, we design two auxiliary methods of communication. The first, named *sensor-based*, uses sensors to obtain information on adjacent vehicles. The second, named *latest-receiving*, uses messages received in the previous frame. For the first method, considering that the sensors are limited to obtaining only current position and velocity information on adjacent vehicles and do not include their acceleration, the predictive information is extended from the sensed measurement assuming that the velocity remains constant in the prediction window. For the second method, if message exchanges with adjacent vehicles fail in the current frame, their information used for control parameter setting is modified from those received in the previous frame by

$$\mathbf{y}_j^{\mathrm{a}}(k|t) = \mathbf{y}_j^{\mathrm{a}}(k+1|t-T), k = 1, 2, ..., N-1 \tag{21a}$$

$$\mathbf{y}_j^{\mathrm{a}}(N|t) = \mathbf{F}_{\mathrm{d}}\left[\mathbf{y}_j^{\mathrm{a}}(N|t-T), \frac{v_j^{\mathrm{a}}(N|t-T) - v_j^{\mathrm{a}}(N-1|t-T)}{T}\right] \tag{21b}$$

where $j \in \{m-1, m+1\}$ is the index of vehicles adjacent to Vehicle m.

E. Adaptive Coefficient

In the optimization problem, parameters $c_{m,\mathrm{a}}$, $c_{m,\mathrm{u}}$, and $c_{m,j}$ are adaptable to the environment, where the former two are Vehicle m's own-state dependent, and the last one is related to other vehicles' information that Vehicle m receives. A vehicle's status error can thus come from its control errors and status errors contained in other vehicles' information. Each vehicle should use the information of vehicles that have a large probability of successfully receiving the leader's information, i.e., vehicles close to the leader. However, the platoon control strategy is different in cases when a vehicle in the platoon is in an abnormal state (i.e., decelerate or accelerate abnormally). Equipped with advanced sensors, vehicles can detect their own abnormal status. Once occurred, such status information is broadcast in the control messages. Other vehicles will adjust their control upon receiving the notification. Depending on whether or not there is a vehicle member in an abnormal state, we classify the platoon state into normal cases and failure cases, and the parameters in both cases are set differently as follows:

1) Normal Case: Both $c_{m,\mathrm{a}}$ and $c_{m,\mathrm{u}}$ should be considered; while for $c_{m,j}$, only front vehicles are considered, and vehicles closer to the leader have a larger weighting factor.

2) Failure Case: If a vehicle decelerates abnormally, its preceding vehicles drive as in the normal case, and for longitudinal control we consider that the latter vehicles follow the abnormal vehicle to decelerate correspondingly. If a vehicle accelerates abnormally, the vehicle directly behind the abnormal vehicle can become a new leader for all the vehicles following behind, and vehicles in front of the abnormal vehicle will accelerate correspondingly to avoid intra-platoon collisions.

VI. Simulation Results

In this section, simulations are conducted to evaluate the proposed joint communication and control scheme. The initial state of the platoon at $t = 0$ is set at a desired state: the leader with $x_0(0) = 10M$ m and $v_0(0) = 20$ m/s, and the follower vehicles with $x_m(0) = 10(M-m)$ m, $v_m(0) = 20$ m/s, and the desired spacing at 10 m. The trajectory of the leader is given by

$$v_0 = \begin{cases} 20 + 0.5t & t \in [0, 8] \text{ s} \\ 24 & t \in (8, 12] \text{ s} \\ 24 - (t-12) & t \in (12, 18] \text{ s} \\ 18 & t \in (18, 22] \text{ s} \\ 18 + 0.5(t-22) & t \in (22, 26] \text{ s} \\ 20 & t \in (26, 30] \text{ s}. \end{cases} \tag{22}$$

Unless otherwise stated, the default values of the proposed scheme parameters are as in Table II. Here, to study the performance of the joint design of platoon communication and control, we also let the platoon undergo different levels of external interference I_{ext}, with a default value of -80 dBW. For the wireless channel, we consider a quasi-static fading-channel environment where the channel gain remains unchanged within a frame but can change independently according to the large-scale path loss and small-scale Rayleigh fading. In addition,the subcarrier setting at the physical layer of the proposed communication scheme is the same as that of the C-V2X protocol [32]. Then, for QPSK modulation with coding rate 0.5, a 2.5-MHz channel bandwidth provides a transmission rate of 2016 bits per transmission opportunity for vehicles in both the LID and FID phases, which is larger than the 190 bytes of a normal packet in periodic vehicle traffic [33]. So, as we use less than a quarter of the time resource in a frame for the intra-platoon communication, we actually consider in the simulation a frame setting of long enough duration to accommodate the potential size of messages in both intra-platoon and inter-platoon communication.

Table II
Simulation Default Parameter Values

Parameter	Value	Parameter	Value
T	50 ms	T_{s}	1 ms
M	20	N	20
N_{LID}	5	N_{FID}	6
W	2.5 MHz	I_{ext}	-80dBW
B	6	γ_{th}	12 dB
N_0	-80 dBW	P_{t}	23 dBm
α	3.5	ϵ	$0.6\mathrm{m/s}$
D_{c}	10 m	$u_{\min}$	$-6\mathrm{m/s}^2$
$F_{\max}$	4196 N	m_{v}	1000 kg
f_{e}	0.02	f_{a}	2.5 $\mathrm{N{\cdot}s^2/m^2}$
v_{th}	40 m/s	$c_{m,\mathrm{a}}$	0.1
$c_{m,\mathrm{u}}$	0.1	$c_{m,j}$	$\frac{1}{j-\min_{j\in S_m(t)}\{j\}+1}$ for $j \le m$

Table III
Simulation Parameter Values For C-V2X Mode 4

Parameter	Value
Packet transmission frequency	20 Hz
Channel bandwidth	10 MHz
Number of sub-channels per sub-frame	4
Number of resource blocks per sub-channel	12
Resource re-selection probaility	0.5
Modulation type	QPSK
Coding rate	0.5

Furthermore, to study the effect of the proposed platoon communication scheme, we compare it with that of C-V2X Mode 4. In C-V2X Mode 4, vehicles autonomously select their resources without the assistance of the cellular infrastructure. To this end, they use the sensing-based semi-persistent scheduling (SPS) scheme specified in Release 14 [34], [35]. The interested reader can refer to [32] for details. For a practical comparison with the proposed communication scheme, the parameters of C-V2X Mode 4 in the simulation are set according to [32], as listed in Table III. It is noteworthy that to be consistent with the third generation partnership project (3GPP) standard, we allow C-V2X Mode 4 to have four times the bandwidth of the proposed communication scheme.

In the simulations, we use three communication network topologies: preceding-following (PF), in which each vehicle only uses the information of the preceding vehicle for control; preceding-leader-following (PLF), in which each vehicle uses the information of the leader and the preceding vehicle; and ALL, in which each vehicle uses all the information that it can obtain from other vehicles. A vehicle position error is the deviation of its actual position from the desired position with respect to the platoon leader or a failed vehicle. We record

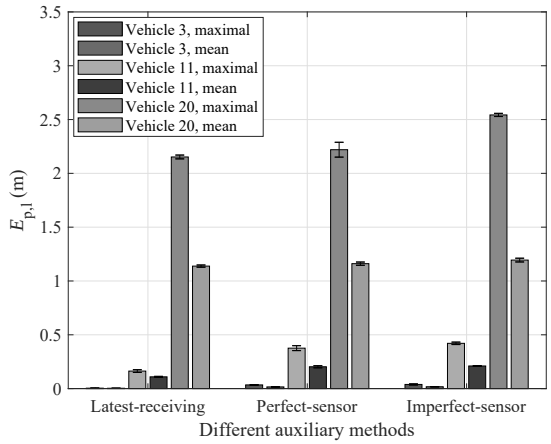

Figure 4. Average position errors with different auxiliary methods of communication under the PF topology.

the position errors at the beginning of each frame and take the maximal and average position errors during the entire control process as the metrics of control performance. The results are averaged over 10 repeated experiments and the confidence interval is set to 95%. Let $E_{\mathrm{p,l}}$ and $E_{\mathrm{p,f}}$ represent the position errors on the basis of the platoon leader in the normal case and of the failed vehicle in the failure cases, respectively. Also, denote $\mathcal{P}_{\mathrm{p}}$ and $\mathcal{P}_{\mathrm{l}}$ as the probability of successfully receiving messages from the preceding vehicle and from the platoon leader, respectively.

To distinguish the effect of sensors, we consider two *sensor-based* methods, namely *perfect-sensor* and *imperfect-sensor*. In the perfect-sensor method, we assume that the obtained data is accurate. In the imperfect-sensor method, the obtained data has measurement errors, where position error and velocity error are set to follow uniform distributions over $[-0.05, 0.05]$ m and $[-0.1, 0.1]$ m/s, respectively. The default auxiliary method is set as *latest-receiving* in the following experiments.

A. PF Topology

Under the PF topology, we perform two experiments in the normal case without using relays. First, we compare the platoon control performance using different auxiliary methods of communication. Fig. 4 shows the average position error under the PF topology for Vehicles 3, 11, and 20. The latter vehicles have larger position errors because their information contains the position error of the preceding vehicles. Therefore, the position errors increase as the number of vehicles increases. Comparing simulation results of the two sensor-based methods, the maximal error is larger if using the imperfect-sensor method, but the average error changes little. This is explainable since the measurement errors have both positive and negative values, generating opposite influences on the platoon control. Thus, through averaging, the effect of measurement errors is reduced. Among the three methods, we find that vehicles using the latest-receiving method has the lowest position errors because it can provide information on predictive frames and acceleration. However, the control

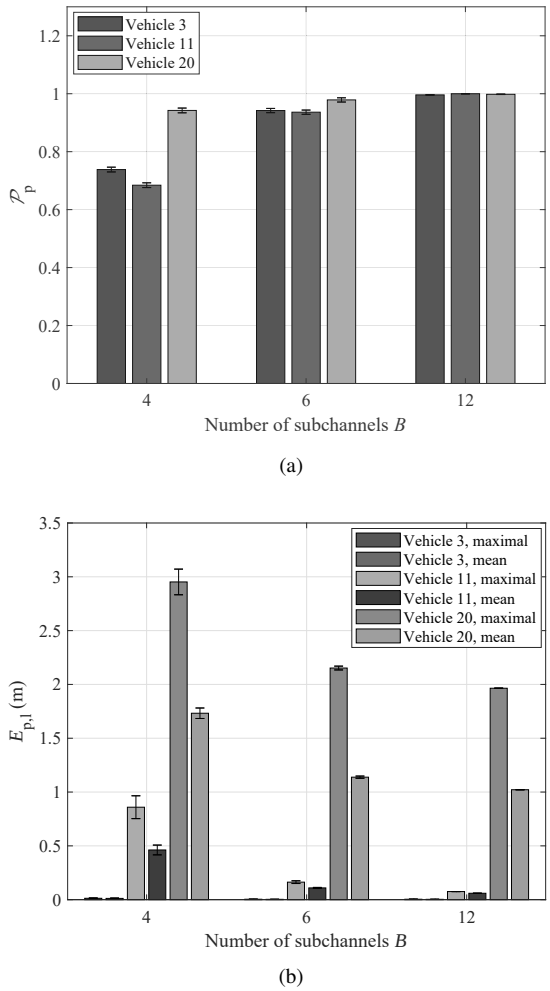

Figure 5. Performance with different numbers of sub-channels under the PF topology. (a) Probability of successfully connecting to the preceding vehicle. (b) Position error of the platoon leader.

performance using the latest-receiving method is largely influenced by the communication environment, which can cause useless out-of-date messages.

The second experiment is conducted to compare the performance with different numbers of sub-channels. Fig. 5 displays the simulation results as the number of sub-channels B varies over 4, 6, and 12. As the number of sub-channels becomes larger, vehicles using the same sub-channel are located further apart. Hence, the probability of successfully receiving the preceding vehicle's information increases. Therefore, the position errors decline, as depicted in Fig. 5(b). This shows that successful connections between vehicles and their preceding vehicles improve platoon control.

B. PLF Topology

In this experiment, we observe the influence of different numbers of slots allocated for LID to analyze the impact of the leader's information. We choose the latest-receiving auxiliary method and set the number of sub-channels to 6. The results are plotted in Fig. 6. It is noteworthy that for the performance comparison in the figure we also show the results

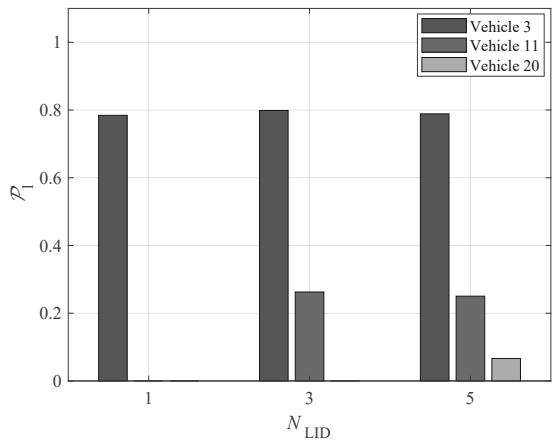

(a)

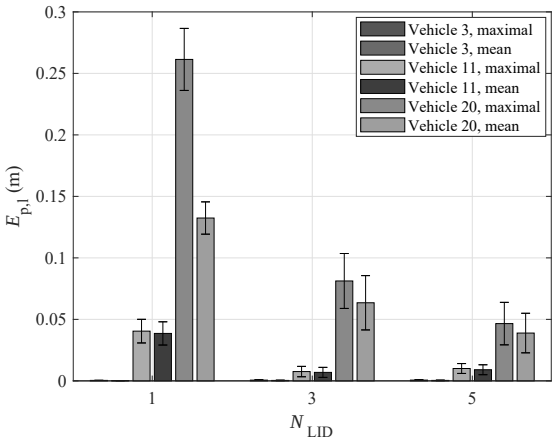

(b)

Figure 6. Performance with different N_{LID}'s under the PLF topology. (a) Probability of successfully connecting to the leader. (b) Position error of the platoon leader.

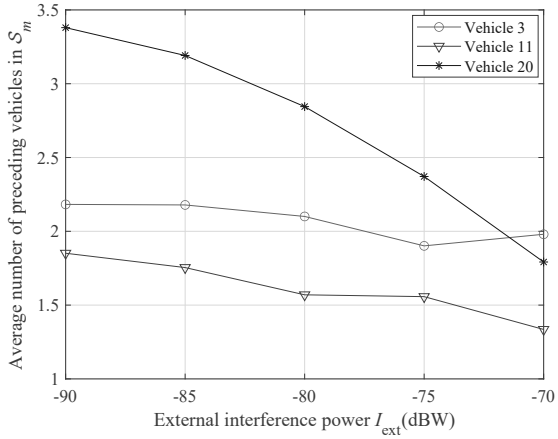

(a)

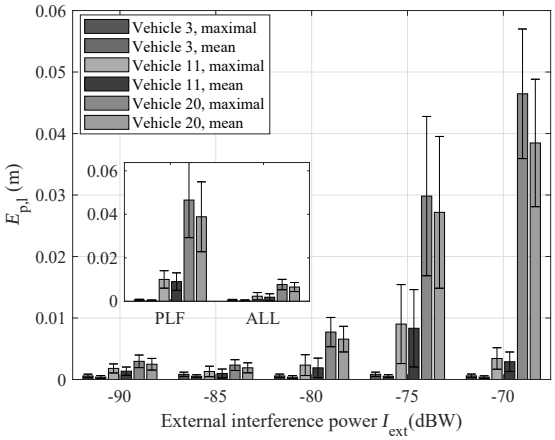

(b)

Figure 7. Performance with different levels of external interference under the ALL topology. (a) Average number of preceding vehicles in $\mathcal{S}_m$. (b) Position error of the platoon leader.

of no activated relay (i.e., $N_{\mathrm{LID}} = 1$). Based on our selection scheme, the selected relays are Vehicles 4 and 8 with $N_{\mathrm{LID}} = 3$ and Vehicles 4, 8, 12, and 16 with $N_{\mathrm{LID}} = 5$, so the result for Vehicle 3 does not change. As N_{LID} or the number of relays grows, $\mathcal{P}_{\mathrm{l}}$ increases significantly for Vehicles 11 and 20. As opposed to the probability of successful communication, the position errors decrease as the number of slots allocated for LID or the number of relays increases. In addition, comparing the result without relays under the PLF topology with that of the same setting under the PF topology, the position error of all vehicles decreases.

C. ALL Topology

Under the ALL topology, each vehicle receives messages from all the other vehicles. However, in the normal case, only the preceding vehicles' information is used for control. Hence, we focus on the trend of the average number of preceding vehicles in $\mathcal{S}_m$ and the position errors when the external interference changes. The external interference is set as $\{-90, -85, -80, -75, -70\}$ dBW, and N_{LID} is set to 5 (thus four relays are used).

As shown in Fig. 7, Vehicle 20 has the largest average number of preceding vehicles in $\mathcal{S}_{20}$ since it is the last vehicle, and likewise has small intra-platoon interference. Also, in general, this average number declines for all vehicles as the external interference increases, while, on the contrary, the position error increases. However, for Vehicle 3, the average number of preceding vehicles in $\mathcal{S}_3$ increases and the position error of Vehicle 11 decreases, when the external interference increases from -75 dBW to -70 dBW. That is because the relay selection changes with different levels of external interference. The selected relay set are Vehicles 3, 6, 9, and 12 with $I_{\mathrm{ext}} = -75$ dBW, and Vehicles 2, 4, 6, and 8 with $I_{\mathrm{ext}} = -70$ dBW. The latter relay selection would more benefit vehicles closer to the platoon leader (including Vehicles 3 and 11). Further, comparing the results under the PLF and ALL topologies with the same parameter values (i.e., $N_{\mathrm{LID}} = 5$ and $I_{\mathrm{ext}} = -80$ dBW), the position errors under the ALL topology decline significantly. This means that receiving more preceding vehicles' information improves the platoon control performance.

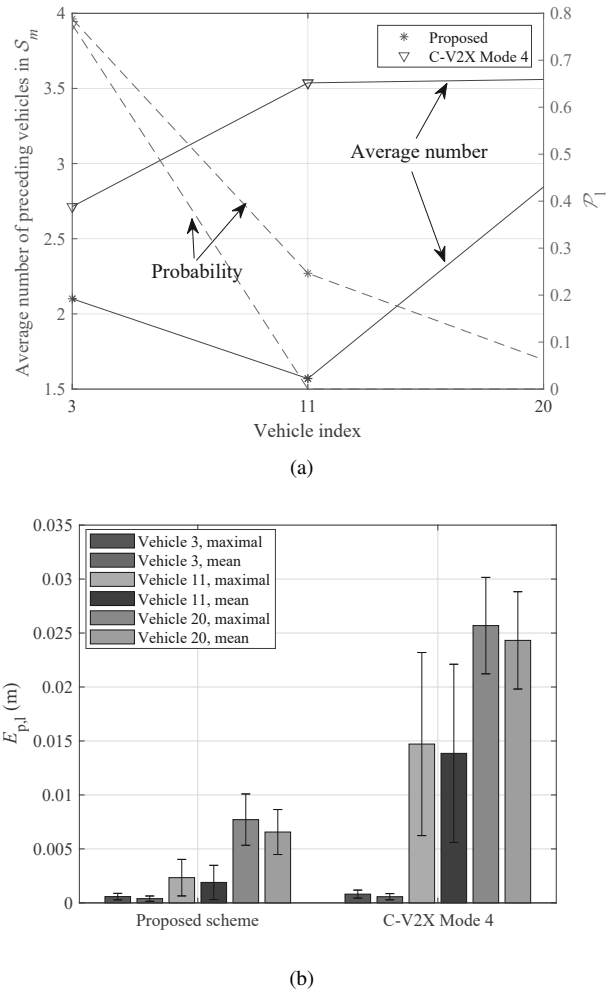

Figure 8. Performance comparison with C-V2X Mode 4. (a) Communication performance. (b) Position error.

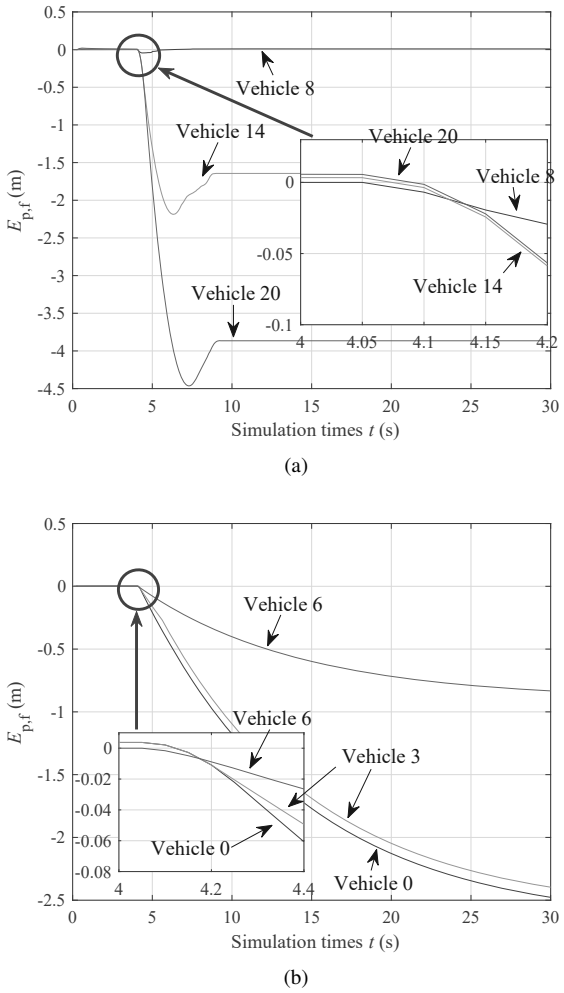

Figure 9. Position errors to the failed vehicle under the ALL topology in failure cases. (a) Deceleration case. (b) Acceleration case.

D. Comparison with C-V2X Mode 4

Fig. 8 shows the performance comparison between our proposed intra-platoon communication scheme and C-V2X Mode 4. From Fig. 8(a) we can see that, using C-V2X Mode 4, vehicles have a larger average number of connectable preceding vehicles due to the fourfold available bandwidth, thus having lower intra-platoon interference. However, as shown in the figure, because of no relay help, vehicles with C-V2X Mode 4 are less probable to connect with the platoon leader. This leads to larger position errors compared with our proposed communication scheme, as shown in Fig. 8(b). Specially, the position error of Vehicle 3 remains almost unchanged because all relays are behind it when $N_{\mathrm{LID}} = 5$, so it does not benefit from deploying relays.

E. Platoon Control in Failure Cases

We conduct simulations of vehicle failure cases consisting of abnormal deceleration and acceleration. In both cases, the control parameters have settings different from Table II, where $c_{m,j}$ is set based on the failure cause. Let Vehicle p be the index of the vehicle in the abnormal state. Then $c_{m,\mathrm{a}}, c_{m,\mathrm{u}}$, and $c_{m,j}$ for each Vehicle m are set as follows. In the deceleration case: if $p < m$, $c_{m,\mathrm{a}}$ and $c_{m,\mathrm{u}}$ are set to 0, and $c_{m,j} = \frac{1}{j-p+1}$ if $p \le j < m$, otherwise $c_{m,j} = 0$; if $p > m$, the setting is the same as with the normal case. In the acceleration case: if $p < m$, Vehicle m moves with the normal parameter setting, following Vehicle $p+1$, which is the new leader for the remaining vehicles; if $p > m$, $c_{m,j} = \frac{1}{p-j+1}$ if $m < j \le p$, otherwise $c_{m,j} = 0$.

The result of the abnormal deceleration case is depicted in Fig. 9(a). At startup, all vehicles move with normal control until $t = 4$ s, when Vehicle 7 breaks down and decelerates at -5 m/s^2. Then, the distances of Vehicles 8, 14, and 20 to the vehicle in the abnormal state decrease. The vehicle in the abnormal state broadcasts its fault indication and Vehicle 8 is the first to obtain notification and take action. So firstly, its position error stops increasing. Then, other vehicles such as Vehicles 14 and 20 behave similarly, as shown in Fig. 9(a). The absolute maximal position error is observed to be 4.5 m at Vehicle 20, which is much smaller than its desired distance gap of 130 m to the vehicle in the abnormal state.

On the other hand, Fig. 9(b) shows the result of the abnormal acceleration case. Vehicle 7 accelerates at $t = 4$ s with its maximal acceleration, and broadcasts its fault indication. The

remaining vehicles separate from the platoon and form a new platoon to drive as normal. So we focus on these preceding vehicles. Vehicle 6 is the closest and firstly obtains the failure information. It then accelerates to keep the desired distance gap. Other vehicles, such as Vehicles 3 and 0, accelerate as well but with different delays, as shown in Fig. 9(b). The position errors of the three vehicles increase through the whole process until these vehicles catch up with the velocity of vehicle in the abnormal state. However, we can see that the maximal absolute position error is less than 2.5 m at 30 s, which is 26 s after Vehicle 7 accelerates abnormally. It is then small enough to avoid collisions. These two experiments demonstrate that with our joint communication and control scheme, collisions can be avoided in failure cases.

VII. Conclusion

In this paper, we have proposed a joint design of platoon communication and control. For the communication part, we focused more on transmitting messages that are useful for platoon control rather than delivering each vehicle's information fairly. The reliability of the leader's information dissemination is improved and the platoon scale is extended through appropriately selecting relays. For the control part, we have designed an adaptive DMPC-based control scheme that can adjust the control parameters according to platoon state and fully utilize all the messages received for better control performance while avoiding collisions. Auxiliary methods of communication have also been adopted to increase the ability of resisting communication failures. Through simulation, we have analyzed the effects of communication on platoon control and tested the safety in platoon failure cases. Simulation results have validated that our proposed scheme can provide good control performance and avoid collision in failure cases.

Appendix A
Derivation of Safe Distance Constraints

Fig. 10(a) illustrates the forward safe distance. Suppose that Vehicle $m-1$ decelerates with $u_{\min}$ in the interval $[t+kT, t+kT+T)$ and stops at time $t_{m-1,\mathrm{f}}$. Then its stop position $x_{m-1}(t_{m-1,\mathrm{f}})$ satisfies

$$x_{m-1}(t_{m-1,\mathrm{f}}) \geq x^{\mathrm{a}}_{m-1}(k|t) - \frac{[v^{\mathrm{a}}_{m-1}(k|t)]^2}{2u_{\min}} \tag{23}$$

where the right side gives the stop position of Vehicle $m-1$ if it starts to decelerate at time $t+kT$.

After Vehicle m receives Vehicle $m-1$'s deceleration report at the next frame, it starts to decelerate with $u_{\min}$ at the second following frame. Supposing that it stops at time $t_{m,\mathrm{f}}$, its stop position $x_m(t_{m,\mathrm{f}})$, given no *a priori* information on future kinetic status, can be estimated as [36]

$$x_m(t_{m,\mathrm{f}}) = x^{\mathrm{p}}_m(k|t) + 2Tv^{\mathrm{p}}_m(k|t) - \frac{[v^{\mathrm{p}}_m(k|t)]^2}{2u_{\min}}. \tag{24}$$

To avoid collisions, we must have $x_{m-1}(t_{m-1,\mathrm{f}}) - x_m(t_{m,\mathrm{f}}) \geq 0$, i.e.,

$$\begin{aligned} x_{m-1}(t_{m-1,\mathrm{f}}) - x_m(t_{m,\mathrm{f}}) \geq & x^{\mathrm{a}}_{m-1}(k|t) - x^{\mathrm{p}}_m(k|t) - 2Tv^{\mathrm{p}}_m(k|t) \\ & - \frac{[v^{\mathrm{a}}_{m-1}(k|t)]^2 - [v^{\mathrm{p}}_m(k|t)]^2}{2u_{\min}} \\ \geq & 0 \end{aligned} \tag{25}$$

which implies that the forward safe distance constraint can be rewritten as

$$\begin{aligned} & x^{\mathrm{a}}_{m-1}(k|t) - x^{\mathrm{p}}_m(k|t) \geq d_{m,\mathrm{f}} \\ & \qquad = 2Tv^{\mathrm{p}}_m(k|t) + \frac{[v^{\mathrm{a}}_{m-1}(k|t)]^2 - [v^{\mathrm{p}}_m(k|t)]^2}{2u_{\min}}. \end{aligned} \tag{26}$$

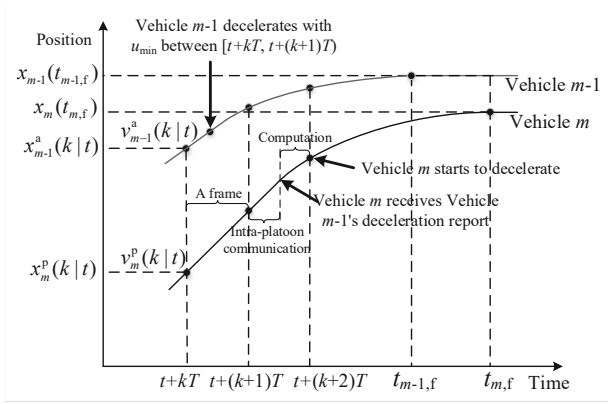

(a)

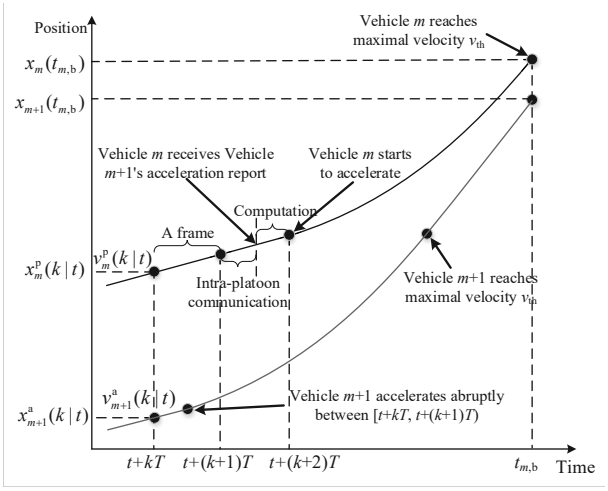

(b)

Figure 10. Safe distance illustration. (a) Forward. (b) Backward.

Fig. 10(b) illustrates the backward safe distance. Consider the worst case, in which Vehicle $m+1$ accelerates abruptly with maximal acceleration in the interval $[t+kT, t+kT+T)$. After Vehicle m receives Vehicle $m+1$'s acceleration report at the following frame, as well at the second following frame, it starts to accelerate with maximal acceleration to avoid a collision. Suppose that after Vehicle $m+1$ reaches the maximal velocity v_{th}, its velocity remains unchanged. Define $t_{m,\mathrm{b}}$ as the time when Vehicle m first reaches v_{th}. Then the position

of Vehicle $m+1$ at time $t_{m,\mathrm{b}}$ satisfies

$$\begin{aligned} x_{m+1}(t_{m,\mathrm{b}}) \leq\ & x^{\mathrm{a}}_{m+1}(k|t) + F_{\mathrm{a},x}[v^{\mathrm{a}}_{m+1}(k|t), v_{\mathrm{th}}] + \\ & \{2T + F_{\mathrm{a},t}[v^{\mathrm{p}}_m(k|t), v_{\mathrm{th}}] - F_{\mathrm{a},t}[v^{\mathrm{a}}_{m+1}(k|t), v_{\mathrm{th}}]\} v_{\mathrm{th}} \end{aligned} \tag{27}$$

where $F_{\mathrm{a},x}(v_{\mathrm{s}}, v_{\mathrm{e}})$ and $F_{\mathrm{a},t}(v_{\mathrm{s}}, v_{\mathrm{e}})$ denote, respectively, vehicle acceleration distance and time from velocity v_{s} to v_{e} with maximal acceleration. Without *a priori* information on future kinetic status, the position $x_m(t_{m,\mathrm{b}})$ when Vehicle m first reaches the maximal velocity can be estimated as [36]

$$x_m(t_{m,\mathrm{b}}) = x^{\mathrm{p}}_m(k|t) + 2T v^{\mathrm{p}}_m(k|t) + F_{\mathrm{a},x}[v^{\mathrm{p}}_m(k|t), v_{\mathrm{th}}]. \tag{28}$$

To avoid a collision, we must have $x_m(t_{m,\mathrm{b}}) - x_{m+1}(t_{m,\mathrm{b}}) \geq 0$. So we have

$$\begin{aligned} & x_m(t_{m,\mathrm{b}}) - x_{m+1}(t_{m,\mathrm{b}}) \\ \geq & \{F_{\mathrm{a},t}[v^{\mathrm{a}}_{m+1}(k|t), v_{\mathrm{th}}] - F_{\mathrm{a},t}[v^{\mathrm{p}}_m(k|t), v_{\mathrm{th}}]\} v_{\mathrm{th}} \\ & + F_{\mathrm{a},x}[v^{\mathrm{p}}_m(k|t), v_{\mathrm{th}}] - F_{\mathrm{a},x}[v^{\mathrm{a}}_{m+1}(k|t), v_{\mathrm{th}}] \\ & + x^{\mathrm{p}}_m(k|t) - x^{\mathrm{a}}_{m+1}(k|t) - 2T[v_{\mathrm{th}} - v^{\mathrm{p}}_m(k|t)] \\ \geq & 0 \end{aligned} \tag{29}$$

which means that the backward safe distance constraint can be written as

$$\begin{aligned} & x^{\mathrm{p}}_m(k|t) - x^{\mathrm{a}}_{m+1}(k|t) \\ \geq & d_{m,\mathrm{b}} \\ = & 2T[v_{\mathrm{th}} - v^{\mathrm{p}}_m(k|t)] + F_{\mathrm{a},x}[v^{\mathrm{a}}_{m+1}(k|t), v_{\mathrm{th}}] - F_{\mathrm{a},x}[v^{\mathrm{p}}_m(k|t), v_{\mathrm{th}}] \\ & + \{F_{\mathrm{a},t}[v^{\mathrm{p}}_m(k|t), v_{\mathrm{th}}] - F_{\mathrm{a},t}[v^{\mathrm{a}}_{m+1}(k|t), v_{\mathrm{th}}]\} v_{\mathrm{th}}. \end{aligned} \tag{30}$$

Appendix B
Simplification of Safe Distance Constraints

For the forward safe distance constraint (15a), as $u_{\min}$ is negative, $d_{m,\mathrm{f}}$ increases with $v^{\mathrm{p}}_m(k|t)$ given $v^{\mathrm{p}}_m(k|t) > 0$. According to (13), before Vehicle $m-1$ decelerates, Vehicles $m-1$ and m move with appropriately maintained velocities, i.e., $v^{\mathrm{p}}_m(k|t) \leq v^{\mathrm{a}}_{m-1}(k|t) + \epsilon$. So by substituting $v^{\mathrm{p}}_m(k|t) = v^{\mathrm{a}}_{m-1}(k|t) + \epsilon$ into (15), we obtain

$$d_{m,\mathrm{f}} \leq 2T v^{\mathrm{p}}_m(k|t) - \frac{2v^{\mathrm{a}}_{m-1}(k|t)\epsilon + \epsilon^2}{2u_{\min}}. \tag{31}$$

For the backward safe distance constraint (15b), we first define two functions. Let $x = f(t)$ and $v = g(t)$ denote, respectively, the time-dependent position and velocity of a vehicle that accelerates with maximal acceleration from $x = 0$ and $v = 0$ at $t = 0$ until reaching the maximal velocity v_{th}. Then, $F_{\mathrm{a},x}(v_{\mathrm{s}}, v_{\mathrm{e}})$ and $F_{\mathrm{a},t}(v_{\mathrm{s}}, v_{\mathrm{e}})$ in (15b) can be expressed as $F_{\mathrm{a},x}(v_{\mathrm{s}}, v_{\mathrm{e}}) = f(t_{\mathrm{e}}) - f(t_{\mathrm{s}})$ and $F_{\mathrm{a},t}(v_{\mathrm{s}}, v_{\mathrm{e}}) = t_{\mathrm{e}} - t_{\mathrm{s}}$, respectively, where $t_{\mathrm{e}} = g^{-1}(v_{\mathrm{e}})$ and $t_{\mathrm{s}} = g^{-1}(v_{\mathrm{s}})$ are the times when the vehicle's velocity is v_{e} and v_{s}, respectively. So, $d_{m,\mathrm{b}}$ in (15b) can be rewritten as

$$\begin{aligned} d_{m,\mathrm{b}} = & 2T[v_{\mathrm{th}} - v^{\mathrm{p}}_m(k|t)] + f\{g^{-1}[v^{\mathrm{p}}_m(k|t)]\} - f\{g^{-1}[v^{\mathrm{a}}_{m+1}(k|t)]\} \\ & + \{g^{-1}[v^{\mathrm{a}}_{m+1}(k|t)] - g^{-1}[v^{\mathrm{p}}_m(k|t)]\} v_{\mathrm{th}}. \end{aligned} \tag{32}$$

Note that to address optimization problem (17) efficiently, the acceleration constraint (14) is replaced with its necessary condition (19). So, a vehicle's maximal acceleration has a linear relationship with its velocity v, i.e., $u_{\max} = Av + u_0$, where $A = \frac{u_{\mathrm{th}} - u_0}{v_{\mathrm{th}}}$. Substituting this into

$$\begin{cases} \dot{f}(t) = g(t) \\ \dot{g}(t) = \dot{v} = u_{\max} \end{cases} \tag{33}$$

with initial conditions $f(0) = 0$ and $g(0) = 0$, we obtain

$$f(t) = \frac{u_0}{A} t + \frac{u_0}{A^2} e^{At} - \frac{u_0}{A^2} \tag{34a}$$

$$g(t) = \frac{u_0}{A}(e^{At} - 1). \tag{34b}$$

Combining (32) and (34), we have

$$\begin{aligned} d_{m,\mathrm{b}} = & 2T[v_{\mathrm{th}} - v^{\mathrm{p}}_m(k|t)] + \frac{1}{A}[v^{\mathrm{p}}_m(k|t) - v^{\mathrm{a}}_{m+1}(k|t)] \\ & - \frac{u_{\mathrm{th}}}{A^2} \left\{ \ln\left[\frac{A}{u_0} v^{\mathrm{p}}_m(k|t) + 1\right] - \ln\left[\frac{A}{u_0} v^{\mathrm{a}}_{m+1}(k|t) + 1\right] \right\} \end{aligned} \tag{35}$$

where the last item decreases with $v^{\mathrm{p}}_m(k|t)$ when $0 \leq v^{\mathrm{p}}_m(k|t) \leq v_{\mathrm{th}}$. According to (13), $v^{\mathrm{p}}_m(k|t) \geq v^{\mathrm{a}}_{m+1}(k|t) - \epsilon$. Then, by substituting $v^{\mathrm{p}}_m(k|t) = v^{\mathrm{a}}_{m+1}(k|t) - \epsilon$ into the last term of (35), we have

$$\begin{aligned} d_{m,\mathrm{b}} \leq & 2T[v_{\mathrm{th}} - v^{\mathrm{p}}_m(k|t)] + \frac{1}{A}[v^{\mathrm{p}}_m(k|t) - v^{\mathrm{a}}_{m+1}(k|t)] \\ & - \frac{u_{\mathrm{th}}}{A^2} \left(\ln\left\{ \frac{A}{u_0} \left[v^{\mathrm{a}}_{m+1}(k|t) - \epsilon\right] + 1 \right\} \right. \\ & \left. - \ln\left[\frac{A}{u_0} v^{\mathrm{a}}_{m+1}(k|t) + 1\right] \right). \end{aligned} \tag{36}$$

Acknowledgment

The authors sincerely thank the anonymous reviewers for their valuable comments that helped improve the readability and clarity of the paper.

References

[1] D. Jia, K. Lu, J. Wang, X. Zhang, and X. Shen, "A survey on platoon-based vehicular cyber-physical systems," *IEEE Commun. Surveys & Tuts.*, vol. 18, no. 1, pp. 263–284, 2016.

[2] B. van Arem, C. J. G. V. Driel, and R. Visser, "The impact of cooperative adaptive cruise control on traffic-flow characteristics," *IEEE Trans. Intell. Transp. Syst.*, vol. 7, no. 4, pp. 429–436, Dec. 2006.

[3] V. Turri, B. Besselink, and K. H. Johansson, "Cooperative look-ahead control for fuel-efficient and safe heavy-duty vehicle platooning," *IEEE Trans. Control Syst. Technol.*, vol. 25, no. 1, pp. 12–28, Jan. 2017.

[4] G. Guo and W. Yue, "Autonomous platoon control allowing range-limited sensors," *IEEE Trans. Veh. Technol.*, vol. 61, no. 7, pp. 2901–2912, Sep. 2012.

[5] Y. W. Le, C. Li, G. Y. Gang, G. Lei, and C. Z. Xu, "State observability and observers of linear-time-invariant systems under irregular sampling and sensor limitations," *IEEE Trans. Autom. Control*, vol. 56, no. 11, pp. 2639–2654, Nov. 2011.

[6] H. Kim, "Application-level frequency control of periodic safety messages in the IEEE WAVE," *IEEE Trans. Veh. Technol.*, vol. 61, no. 4, pp. 1854–1862, May 2012.

[7] Y. Fan and S. Biswas, "Self-configuring TDMA protocols for enhancing vehicle safety with DSRC based vehicle-to-vehicle communications," *IEEE J. Sel. Areas Commun.*, vol. 25, no. 8, pp. 1526–1537, Oct. 2007.

[8] L. Sun, A. Huang, H. Shan, and C. Lin, "Adaptive beaconing for collision avoidance and tracking accuracy in vehicular networks," in *Proc. IEEE WCNC*, Mar. 2017, pp. 1–6.

[9] Y. Bi, H. Shan, X. Shen, W. Ning, and Z. Hai, "A multi-hop broadcast protocol for emergency message dissemination in urban vehicular ad hoc networks," *IEEE Trans. Intell. Transp. Syst.*, vol. 17, no. 3, pp. 736–750, Mar. 2016.

[10] M. Torrent-Moreno, J. Mittag, P. Santi, and H. Hartenstein, "Vehicle-to-vehicle communication: Fair transmit power control for safety-critical information," *IEEE Trans. Veh. Technol.*, vol. 58, no. 7, pp. 3684–3703, Sep. 2009.

[11] M. Segata, F. Dressler, and R. L. Cigno, "Jerk beaconing: A dynamic approach to platooning," in *Proc. IEEE VNC*, Dec. 2015, pp. 135–142.

[12] R. Wang, J. Wu, and J. Yan, "Resource allocation for D2D-enabled communications in vehicle platooning," *IEEE Access*, vol. 6, pp. 50526–50537, Sep. 2018.

[13] L. Xu, L. Y. Wang, G. Yin, and H. Zhang, "Communication information structures and contents for enhanced safety of highway vehicle platoons," *IEEE Trans. Veh. Technol.*, vol. 63, no. 9, pp. 4206–4220, Nov. 2014.

[14] S. Oncu, J. Ploeg, N. V. D. Wouw, and H. Nijmeijer, "Cooperative adaptive cruise control: Network-aware analysis of string stability," *IEEE Trans. Intell. Transp. Syst.*, vol. 15, no. 4, pp. 1527–1537, Aug. 2014.

[15] P. Fernandes and U. Nunes, "Platooning with IVC-enabled autonomous vehicles: Strategies to mitigate communication delays, improve safety and traffic flow," *IEEE Trans. Intell. Transp. Syst.*, vol. 13, no. 1, pp. 91–106, Mar. 2012.

[16] J. W. Kwon and D. Chwa, "Adaptive bidirectional platoon control using a coupled sliding mode control method," *IEEE Trans. Intell. Transp. Syst.*, vol. 15, no. 5, pp. 2040–2048, Oct. 2014.

[17] E. Kayacan, "Multi-objective H_∞ control for string stability of cooperative adaptive cruise control systems," *IEEE Trans. Intell. Veh.*, vol. 2, no. 1, pp. 52–61, Mar. 2017.

[18] J. Ploeg, D. P. Shukla, N. van de Wouw, and H. Nijmeijer, "Controller synthesis for string stability of vehicle platoons," *IEEE Trans. Intell. Transp. Syst.*, vol. 15, no. 2, pp. 854–865, Apr. 2014.

[19] W. B. Dunbar and D. S. Caveney, "Distributed receding horizon control of vehicle platoons: Stability and string stability," *IEEE Trans. Autom. Control*, vol. 57, no. 3, pp. 620–633, Mar. 2012.

[20] R. Kianfar, B. Augusto, A. Ebadighajari, U. Hakeem, J. Nilsson, A. Raza, R. S. Tabar, V. K. Irukulapati, C. Englund, and P. Falcone, "Design and experimental validation of a cooperative driving system in the grand cooperative driving challenge," *IEEE Trans. Intell. Transp. Syst.*, vol. 13, no. 3, pp. 994–1007, Sep. 2012.

[21] Z. Yang, S. E. Li, J. Wang, D. Cao, and K. Li, "Stability and scalability of homogeneous vehicular platoon: Study on the influence of information flow topologies," *IEEE Trans. Intell. Transp. Syst.*, vol. 17, no. 1, pp. 14–26, Jan. 2016.

[22] S. E. Li, Y. Zheng, K. Li, and J. Wang, "An overview of vehicular platoon control under the four-component framework," in *Proc. IEEE Intelligent Vehicles Symposium*, Jun. 2015, pp. 286–291.

[23] B. Liu, D. Jia, K. Lu, N. Dong, J. Wang, and L. Wu, "A joint control-communication design for reliable vehicle platooning in hybrid traffic," *IEEE Trans. Veh. Technol.*, vol. 66, no. 10, pp. 9394–9409, Oct. 2017.

[24] C. Zhang, Y. Zang, J. A. Leon Calvo, and R. Mathar, "A novel V2V assisted platooning system: Control scheme and MAC layer designs," in *Proc. IEEE PIMRC*, Oct. 2017, pp. 1–7.

[25] J. Mei, K. Zheng, L. Zhao, L. Lei, and X. Wang, "Joint radio resource allocation and control for vehicle platooning in LTE-V2V network," *IEEE Trans. Veh. Technol.*, vol. 67, no. 12, pp. 12 218–12 229, Dec. 2018.

[26] H. Peng, D. Li, Y. Qiang, K. Abboud, and X. Shen, "Resource allocation for cellular-based inter-vehicle communications in autonomous multiplatoons," *IEEE Trans. Veh. Technol.*, vol. 66, no. 12, pp. 11 249–11 263, Dec. 2017.

[27] H. Peng, D. Li, K. Abboud, H. Zhou, Z. Hai, W. Zhuang, and X. Shen, "Performance analysis of IEEE 802.11p DCF for multiplatooning communications with autonomous vehicles," *IEEE Trans. Veh. Technol.*, vol. 66, no. 3, pp. 2485–2498, Mar. 2017.

[28] L. Xiao and F. Gao, "Practical string stability of platoon of adaptive cruise control vehicles," *IEEE Trans. Intell. Transp. Syst.*, vol. 12, no. 4, pp. 1184–1194, Dec. 2011.

[29] Y. Zheng, S. E. Li, K. Li, F. Borrelli, and J. K. Hedrick, "Distributed model predictive control for heterogeneous vehicle platoons under unidirectional topologies," *IEEE Trans. Control Syst. Technol.*, vol. 25, no. 3, pp. 899–910, May 2017.

[30] T. H. Cormen, C. E. Leiserson, R. L. Rivest, and C. Stein, *Introduction to Algorithms*. MIT Press, 2009.

[31] S. Boyd and L. Vandenberghe, *Convex Optimization*. Cambridge University Press, 2004.

[32] M. Gonzalez-Martin, M. Sepulcre, R. Molina-Masegosa, and J. Gozalvez, "Analytical models of the performance of C-V2X mode 4 vehicular communications," *IEEE Trans. Veh. Technol.*, vol. 68, no. 2, pp. 1155–1166, Feb. 2017.

[33] 3GPP TR 36.885, "Study on LTE-based V2X services," Release 14 V14.0.0, Jul. 2016.

[34] 3GPP TS 36.213, "Evolved universal terrestrial radio access (E-UTRA); physical layer procedures," Release 14 V14.3.0, Jun. 2017.

[35] 3GPP TS 36.321, "Evolved universal terrestrial radio access (E-UTRA); medium access control (MAC) protocol specification," Release 14 V14.3.0, Jun. 2017.

[36] Y. Lian, Y. Zhao, L. Hu, and Y. Tian, "Longitudinal collision avoidance control of electric vehicles based on a new safety distance model and constrained-regenerative-braking-strength-continuity braking force distribution strategy," *IEEE Trans. Veh. Technol.*, vol. 65, no. 6, pp. 4079–4094, Jun. 2016.